Chemical Engineering Journal 147 (2009) 173–179

Contents lists available at ScienceDirect

Chemical Engineering Journal

journal homepage: www.elsevier.com/locate/cej

Cadmium(II) removal from aqueous solution using microporous titanosilicate ETS-4

Telmo R. Ferreira[a], Cláudia B. Lopes[b], Patrícia F. Lito[a], Marta Otero[b], Zhi Lin[a], João Rocha[a], Eduarda Pereira[b], Carlos M. Silva[a,*], Armando Duarte[b]

[a] CICECO, Department of Chemistry, University of Aveiro, 3810-193 Aveiro, Portugal
[b] CESAM, Department of Chemistry, University of Aveiro, 3810-193 Aveiro, Portugal

ARTICLE INFO

Article history:
Received 11 March 2008
Received in revised form 9 June 2008
Accepted 28 June 2008

Keywords:
ETS-4
Cadmium(II)
Ion exchange
Nernst–Planck
Batch experiments

ABSTRACT

The ability of microporous titanosilicate ETS-4 to uptake Cd^{2+} from aqueous solutions has been investigated, assessing its potential in water remediation. In order to study the equilibrium and the kinetics of the process, batch stirred tank experiments have been carried out by contacting a fixed volume of solution with known masses of ETS-4. The evolution of the cadmium concentration with time has been monitored by inductively coupled plasma mass spectrometry. Concerning equilibrium, Freundlich isotherm performs accurately in the range of experimental conditions studied. The solid loadings measured in this essay surmount significantly the values found in literature for different ion exchangers in the same range of temperatures. A Nernst–Planck based model combining internal and external diffusion resistances has been used to describe the ion exchange process, where the convective mass transfer coefficient and the self-diffusivities of the counter ions are the unique parameters. The Nernst–Planck based model accomplishes good representations (average absolute deviation of 6.74%), even in the transition from the steep descent to the horizontal branch of the bulk concentration *versus* time curve. The results obtained using the commonly adopted pseudo first- and second-order models found in literature are worse (average absolute deviation of 215.7% and 12.11%, respectively), although more parameters are involved.

1. Introduction

It is widely known that heavy metals present in superficial waters are extremely dangerous to environmental and human health because they are not biodegradable and must be removed to prevent their accumulation. Industrial discharges, mainly from mining, metal finishing, welding, alloys manufacturing plants, pulp industries and petroleum refining, are responsible for heavy metal contamination [1]. Cadmium is one of the most toxic non-essential heavy metals present in the environment, even at low concentrations. Therefore, removal of trace levels of cadmium is required.

Several methods are available to remove toxic metals from aqueous waste streams, such as chemical precipitation, electrolysis (membrane separation), and ion exchange. The latter is probably one of the most attractive processes and, consequently, the commonly used in industry, because of its simple and efficient application. However, the cost and the regeneration of the adsorbent are limiting factors [2], hence it is of interest to research new materials to replace expensive activated carbons and resins. Natural and synthetic zeolites are gaining considerable interest because of their high selective and ion-exchange capacity [3–7].

Generally, microporous titanosilicates are three-dimensional crystalline solids with a well-defined structure containing titanium, silicon and oxygen atoms [8]. These materials have a regular crystalline framework formed by a three-dimensional combination of tetrahedral and octahedral building blocks connected with each other by shared oxygen atoms. Each TiO_6 octahedron in the titanosilicate global structure carries a −2 charge, which can be neutralized by extra-framework cations (e.g., Na^+ and K^+). These compensation species, as well as water molecules or other adsorbed molecules, are located in the channels of the structure and can be replaced by others. Titanosilicates exhibit remarkable physical and chemical properties, such as selective sorption, ion exchange and catalytic activity [8]. Of special importance for environmental uses is their ability to uptake and retain heavy metal species from aqueous media. ETS-4 (Engelhard Titanium Silicates No. 4) contains octahedral and square-pyramidal titanium units, in addition to the tetrahedral silicate units. The 12-ring channels are separated by the 8 ring windows. ETS-4 has been suggested as good ion exchanger [8].

* Corresponding author at: Department of Chemistry, University of Aveiro, Campus Universitário de Santiago, 3810-193 Aveiro, Portugal. Tel.: +351 234 401549; fax: +351 234 370084.
E-mail address: carlos.manuel@ua.pt (C.M. Silva).

1385-8947/$ – see front matter © 2008 Elsevier B.V. All rights reserved.
doi:10.1016/j.cej.2008.06.032

Nomenclature

AAD	average absolute deviation (%)
C_A	concentration of A in bulk solution (mol/m^3)
d_p	particle diameter (m)
D_{Aw}	diffusivity of the solute in solution (m^2/s)
D_A,D_B	self-diffusion coefficient of species A and B (m^2/s)
D_{AB}	interdiffusion coefficient of the pair A–B (m^2/s)
k_1	first-order sorption rate constant in Eq. (15) (s^{-1})
k_2	second-order rate constant in Eq. (16) (m^3/(s mol))
k_f	convective mass transfer coefficient (m/s)
K_F	Freundlich parameter (Eq. (11))
K_L	Langmuir parameter (Eq. (12))
m_{ETS-4}	mass of ETS-4 (kg)
n	Freundlich parameter (Eq. (11))
N_A	intraparticle molar flux of species A (mol/m^2 s)
q_A,q_B	molar concentration of counter ions A and B in the particle (mol/m^3)
$\bar{q}_A$	average concentration of counter ion A in the particle (mol/m^3)
q_{max}	maximum ion exchanger capacity (mol/m^3)
r	radial position in the particle (m)
R	particle radius, m; % of ion removed relative to equilibrium limit concentrations
Re	Reynolds number ($= \varepsilon^{1/3} d_p^{4/3}/\nu$)
Sc	Schmidt number ($=\nu/D$)
Sh	Sherwood number ($=k_f d_p/D$)
t	time (s) (and h in figures)
t_{st}	stoichiometric time (s)
V_L	volume of solution (m^3)
V_{ETS-4}	volume of ETS-4 (m^3)
z_A,z_B	charges of components A and B

Greek letters

ε	bed porosity; mixer power input per unit of fluid mass (m^2/s^3)
ν	kinematic viscosity (m^2/s)
ρ_{ETS-4}	density of ETS-4 (kg/m^3)
τ	space-time (s)

Subscripts

A	counter ion initially present in bulk solution (Cd^{2+})
B	counter ions initially present in particle (Na^+)
eq	final equilibrium condition of experiment
f	feed condition
0	initial condition of experiment
s	solid–liquid solution interface

The kinetics of ion exchange is frequently correlated using semiempirical pseudo first- and second-order equations [9–11]. However, such models are merely correlative, which limits their application and extrapolation. An alternative approach adopts Nernst–Planck equations to describe mass transport in ionic systems, accounting for concentration and electric potential gradients induced by the different counter ions mobility [7,12,13].

In previous works [6,7,14,15] we studied the applicability of titanosilicate ETS-4 to uptake Hg^{2+} cation from aqueous solution and good results have been found.

In this essay we evaluate the ability of microporous titanosilicate ETS-4 to remove Cd^{2+} ions from aqueous solution, assessing its potential as a decontaminating agent. The results of the batch experiments performed are modelled using Nernst–Planck equations. Classical pseudo first- and second-order models are also included for comparison.

Table 1
Features of the ETS-4 particles used

Formula	$[Na_9Ti_5Si_{12}O_{38}(OH)\cdot 12H_2O]$
Density (kg/m^3)	2200
Ion-exchanger capacity (equiv./kg)	6.39
Particle diameter ($\times 10^{-6}$ m)	0.5–0.9
Pore diameter ($\times 10^{-10}$ m)	3–4

2. Experimental

2.1. Materials and solutions

2.1.1. Chemicals

All chemicals used were of analytical reagent grade and obtained from commercial suppliers without further purification. The certified standard stock solution of cadmium (1001 ± 2 mg L^{-1}) was purchased from Merck.

2.1.2. ETS-4

The synthesis of ETS-4 was performed as follows: an alkaline solution was made by dissolving 33.16 g of metasilicate (BDH), 2.00 g NaOH (Merck), and 3.00 g KCl (Merck) into 25.40 g H_2O. 31.88 g of $TiCl_3$ (15% (w/w) $TiCl_3$ and 10% (w/w) HCl, Merck) were added to this solution and stirred thoroughly. This gel, with a molar composition $5.9Na_2O{:}0.7K_2O{:}5.0SiO_2{:}1.0TiO_2{:}114H_2O$, was transferred to a Teflon-lined autoclave and treated at 230 °C for 17 h under autogenous pressure without agitation. The product was filtered off, washed at room temperature with distilled water, and dried at 70 °C overnight, the final product being an off-white microcrystalline powder. Table 1 summarises relevant features of the zeolite particles [16].

2.1.3. Inactivation of glass surface

All glassware used in the experiments were acid-washed prior to use (nitric acid 25%, 12 h followed by hydrochloric acid 25% another 12 h).

2.1.4. Cadmium solutions

Cadmium solutions were prepared daily by diluting the stock solution to the desired concentrations in high purity water (18 MΩ cm). The stock solution of cadmium(II) is extremely acidic and when it is diluted in 2 L of water, a solution with a pH value of around 4 is obtained. The pH value remains approximately constant during the experiments avoiding the addition of any buffer solution.

2.2. Experiments

All experiments were carried out in batch conditions, at 295 ± 1 K in a 2 L volumetric flask. Known masses of ETS-4 were added to the cadmium solutions and this time was considered the starting point of the experiment. Table 2 depicts the experimental

Table 2
Experimental conditions for isothermal batch operation

Experimental conditions	Exp. 1	Exp. 2	Exp. 3	Exp. 4
Temperature (K)	295 ± 1			
pH (approximately constant during experiment)	4			
Solution volume ($\times 10^{-3}$ m^3)	2			
Initial Cd^{2+} concentration ($\times 10^{-3}$ kg/m^3)	0.84	0.64	0.44	0.62
Mass of ETS-4 ($\times 10^{-6}$ kg)	51	50	51	100

conditions including the initial solution concentrations and ETS-4 masses.

ETS-4 powders and aqueous solutions were maintained in contact under constant stirring. The time required for solution-solid equilibration was evaluated by carrying out each experiment until the Cd^{2+} concentration remained constant. During this period of time, several aliquots (10 mL) were taken at different times and each aliquot was filtered through a 0.45 μm Acetate Plus Osmonics filter. The filtrate was adjusted to pH < 2 with HCl, stored at 277.15 K and then analysed. Besides, a new experiment was carried out in order to obtain an additional equilibrium point. With this purpose, a solution with initial Cd^{2+} concentration of 0.865×10^{-3} kg/m^3 was contacted with 51 mg of ETS-4 until the equilibrium was attained. A blank experiment (without ETS-4) was always run as a control, to check that the removal of cadmium occurred by ion exchange onto ETS-4 and not by, e.g., adsorption on the vessel walls.

Cadmium analysis was performed by inductively coupled plasma mass spectrometry, on a Thermo ICP-MS X Series equipped with a Burgener nebuliser.

The average concentration of sorbed metal at time t, $\bar{q}_A$, was calculated by material balance:

$$\bar{q}_A = \frac{(C_{A0} - C_A)V_L}{V_{ETS\text{-}4}} \quad (1)$$

where the subscript 'A' denotes Cd^{2+}, C_{A0} the initial concentration in solution, C_A the concentration in solution at time t, V_L the solution volume, and $V_{ETS\text{-}4} = m/\rho_{ETS\text{-}4}$ is the volume of ETS-4, m is the mass of ETS-4, and $\rho_{ETS\text{-}4}$ is the ETS-4 density. Furthermore, the percentage of cadmium removed relative to the final equilibrium concentration, $C_{A,eq}$, was also determined:

$$R = \frac{C_{A0} - C_A}{C_{A0} - C_{A,eq}} \times 100 \quad (2)$$

3. Modelling

Ion exchange may be represented by conventional chemical equilibrium [12]. For the case where the zeolite is initially in B (Na^+) form and the counter ion in solution is A (Cd^{2+}), the reaction is

$$z_A\overline{B^{z_B}} + z_B A^{z_A} \Leftrightarrow z_B\overline{A^{z_A}} + z_A B^{z_B} \quad (3)$$

where z_A and z_B are the electrochemical valences.

The Nernst–Planck based model adopted in this work to describe the batch ion exchange considers: (i) film and intraparticle mass transfer resistances; (ii) spherical solid particles; (iii) perfectly stirred tank; (iv) isothermal and isobaric operation; (v) co-ions are excluded from the zeolite particles (Donnan exclusion); and (vi) ideal solution behaviour. The model has been already presented in detail in a previous publication [7] dealing with Hg^{2+} removal from aqueous solution using ETS-4. Hence, only the final set of equations is compiled in Table 3, where q_A and q_B are the molar concentrations of counter ions, $q_{A,eq}$ the final equilibrium concentration, r the radial position, k_f the convective mass transfer coefficient, subscript s refers to surface, D_A and D_B the self-diffusion coefficients of A and B, and D_{AB} is one coupled interdiffusion coefficient. k_1 and k_2 are the kinetic constants of the pseudo first- and second-order models adopted for comparison.

With respect to the equilibrium representation, the Freundlich and Langmuir isotherms have been examined in this work (Eqs. (11) and (12) in Table 3), in the very same way as many researchers do for several materials, especially zeolites [17–20]. Accordingly, K_F and n are the parameters of the Freundlich isotherm, and K_L and q_{max} are the Langmuir parameters.

The simultaneous solution of the model equations gives the concentration of the Cd^{2+} in water, and its concentration profiles in the solid phase as function of position and time. The model has been solved numerically using the Method of Lines [21] and integrated using the Finite-Difference approach. For this purpose, a programme in Matlab has been written to solve the resulting ordinary differential equations (ODEs) with 101 grid points. An odd number of grid points is required when the average loading (Eq. (6)) is numerically evaluated using the 1/3 Simpson's Rule. Ode15s solver has been used to integrate this set of ODEs of the initial-value type.

Table 3
Mathematical models equations

Material balances	$\left(\frac{\partial q_A}{\partial t}\right) = -\frac{1}{r^2}\frac{\partial}{\partial r}(r^2 N_A)$	(4)
	$\frac{\partial C_A}{\partial t} = -\frac{V_{ETS\text{-}4}}{V_L}\frac{\partial \bar{q}_A}{\partial t}$	(5)
	$\bar{q}_A = \frac{3}{R_p^3}\int_0^R r^2 q_A \, dr$	(6)
Initial and boundary conditions	$t = 0, \quad \begin{cases} q_A = \bar{q}_A = 0 \\ C_A = C_{A0} \end{cases}$	(7)
	$r = R, \quad q_A = q_{A,R}$	(8)
	$r = 0, \quad \left(\frac{\partial q_A}{\partial r}\right) = 0$	(9)
Equality of internal and film ionic fluxes	$\left(\frac{\partial q_A}{\partial r}\right)_{r=R} = \frac{k_f}{D_{AB}}(C_A - C_{As})$	(10)
Freundlich isotherm	$q_{A,eq} = K_F C_{A,eq}^{1/n}$	(11)
Langmuir isotherm	$q_{A,eq} = \frac{q_{max} K_L C_{A,eq}}{1 + K_L C_{A,eq}}$	(12)
Nernst–Planck equation for two counter ions in Fick's law form	$N_A = -D_{AB}\left(\frac{\partial q_A}{\partial r}\right)$	(13)
	$D_{AB} \equiv \frac{D_A D_B (z_A^2 q_A + z_B^2 q_B)}{D_A z_A^2 q_A + D_B z_B^2 q_B}$	(14)
Pseudo first-order model	$\log(q_{A,eq} - \bar{q}_A) = \log(\bar{q}_A) - \frac{k_1}{2.303} t$	(15)
Pseudo second-order model	$\frac{t}{\bar{q}_A} = \frac{1}{k_2 q_{A,eq}^2} + \frac{1}{q_{A,eq}} t$	(16)

The self-diffusion coefficients and the convective mass transfer coefficient are the model parameters to fit to the experimental data. Accordingly, a first optimisation step was performed based on the 'elimination of linear parameters in nonlinear regression' technique due to Lawton and Sylvestre [22]. With this procedure, a reduction of the number of parameters that must be estimated by the iterative procedure is achieved, as well as faster convergence attained. Thus, only two initial guesses have to be provided instead of three: specifically the diffusivities ratio D_A/D_B, and k_f. Finally, an enhancing optimisation involving all parameters simultaneously was performed, where the results previously obtained from the above-mentioned technique were taken as reliable initial guesses. This optimisation technique has been successfully applied elsewhere [22,23].

For well established agitated systems, k_f may be predicted using correlations which depend generally on the Reynolds, Schmidt and Power numbers, and on geometrical parameters such as the ratio of impeller to tank diameter, the specific geometry of the impeller, and the geometry of baffling, if any, used to inhibit vortex formation in the vessel. For the particular geometry of our sorption set-up no correlation is available in the literature. Nonetheless, the correlation of Armenante and Kirwan [24] has been adopted to estimate the convective mass transfer coefficient at least to predict its order of magnitude:

$$Sh = 2 + 0.52 Re^{0.52} Sc^{1/3} \quad (17)$$

where $Sh = k_f d_p/D_{Aw}$ is the Sherwood number, d_p the particle diameter, D_{Aw} the diffusivity of the solute in solution, $Re = \varepsilon^{1/3} d_p^{4/3}/\nu$ the

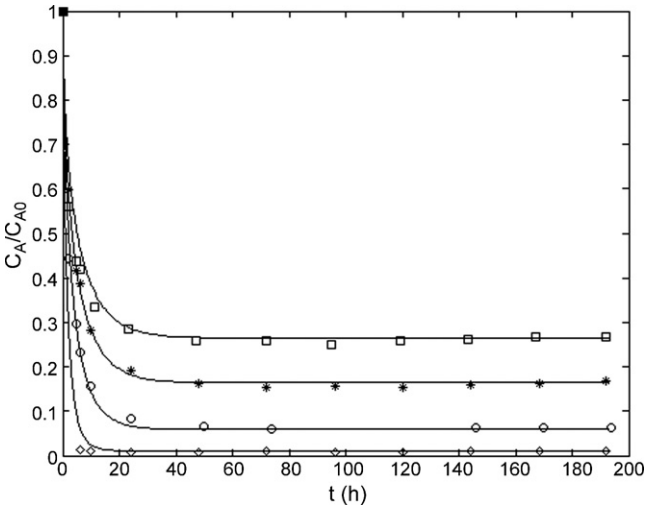

Fig. 1. Normalized concentration of bulk solution *versus* time: modelling (lines; AAD = 6.74%) and experimental data. Experimental conditions (see Table 2): (□) Exp. 1; (*) Exp. 2; (◯) Exp. 3; (◊) Exp. 4.

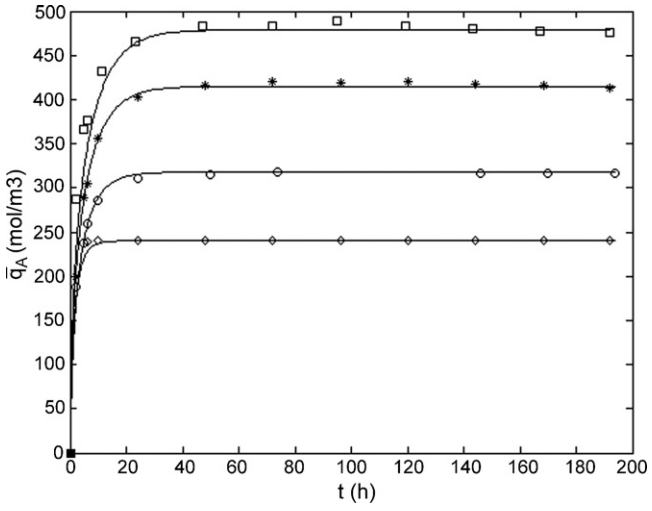

Fig. 2. Average Cd^{2+} concentration in ETS-4 *versus* time: modelling and experimental data. Experimental conditions (see Table 2): Symbols: same as Fig. 1.

Reynolds number, ε the mixer power input per unit of fluid mass, ν the kinematic viscosity, and $Sc = \nu/D_{Aw}$ is the Schmidt number. This equation is frequently applied to fix k_f in the model equations or, alternatively, to estimate k_f and compare it with the optimized value from experimental data [25,26].

4. Results and discussion

Fig. 1 shows the normalized Cd^{2+} concentration in the fluid as a function of time, measured for different initial solution concentrations and/or ETS-4 masses, i.e. $C_A/C_{A0} = f(t; C_{A0}, m_{ETS\text{-}4})$. Fast metal uptake occurs in the first few hours of the process for all the experimental conditions, followed by the characteristic slower removal towards the equilibrium. The horizontal branch of each curve was used to determine the equilibrium isotherm. In order to enlarge its range of applicability, an additional experiment was carried out to obtain a new data point (for initial concentration 0.865×10^{-3} kg/m^3 and 51 mg of ETS-4), for which only equilibrium concentrations were measured (between 80 and 190 h). For this reason, the respective transient data are absent in Fig. 1. In Fig. 2 the average concentration of Cd^{2+} inside the particle is represented along time. It is important to focus that calculated results are much better when such concentration is used instead of that in bulk solution. However, in this work all deviations are calculated from solution concentrations, as these are the ones that we really measured experimentally. As it was expected in advance the results in Figs. 1 and 2 complement each other, as they are linked by material balance (see Eq. (1)).

In Fig. 3 the percentage of cadmium(II) removed relative to the final equilibrium concentration as a function of time is plotted. Accordingly, 20 h are enough to eliminate ca. 97% of cadmium(II) in Exp. 1, 2 and 3. Moreover, after 10 h of contact, 85% of Cd^{2+} has already been removed. When 100 mg of ETS-4 are used (Exp. 4), 94% of Cd^{2+} is eliminated in only 2 h. This last case corresponds to 50 g of ETS-4 per m^3 of solution, and initial concentration 0.62×10^{-3} kg/m^3.

In this work, the equilibrium was found to be well represented by the Freundlich isotherm. Fig. 4 shows experimental data along with calculated results:

$$q_{A,eq}(\text{equiv./m}^3) = 2639.37(C_{A,eq}(\text{equiv./m}^3))^{1/5.51} \quad (18)$$

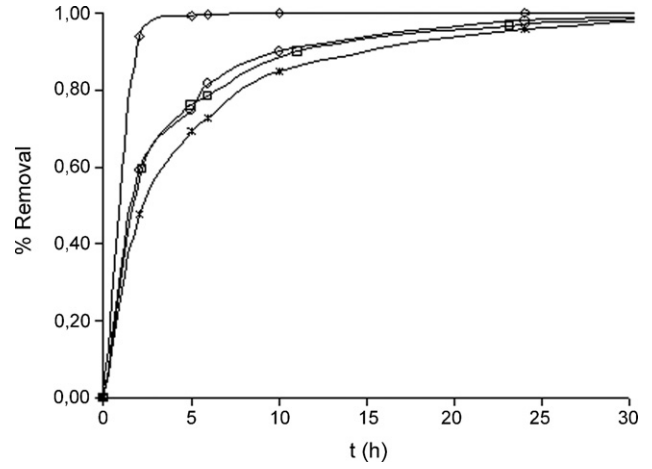

Fig. 3. Percentage of cadmium(II) removed relative to the final equilibrium concentration as a function of time, for the first 30 h of the experiments. Experimental conditions (see Table 2): (□) Exp. 1; (*) Exp. 2; (◯) Exp. 3; (◊) Exp. 4.

This isotherm fits data accurately in the range of experimental conditions studied: AAD = 2.18% and the correlation coefficient is 0.9988. On the contrary, Langmuir model gives rise to AAD = 9.58%, where AAD is the usual average absolute deviation. Furthermore, it is worth noting that Langmuir predicts a maximum corresponding

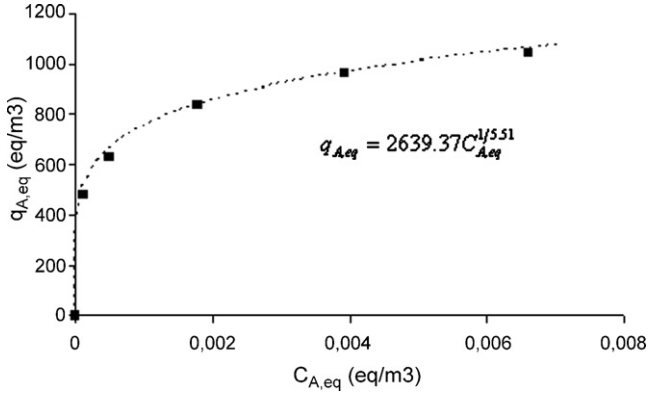

Fig. 4. Equilibrium experimental data and Freundlich isotherm fitted. $T = 295$ K. AAD = 2.18% and correlation coefficient = 0.9988.

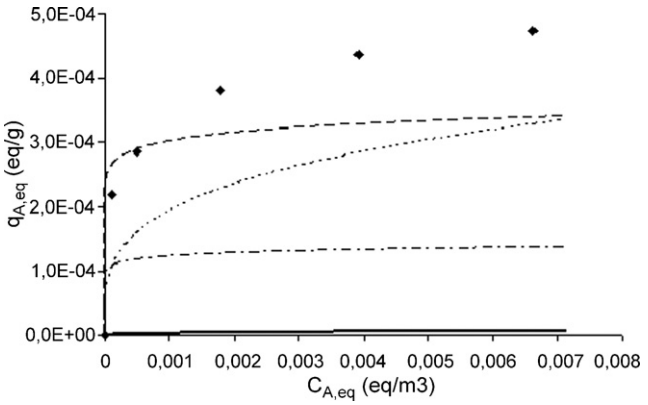

Fig. 5. Comparison between equilibrium data measured in this work (ETS-4, 295 K; lozenges) and other isotherms available in literature for different solid materials: dashed and dash-dotted lines, Amberlite IR 120 and dolomite (293 K) [17]; dotted line, synthetic zeolite A (298 K) [18]; solid thick line, clinoptilolite (room temperature) [19].

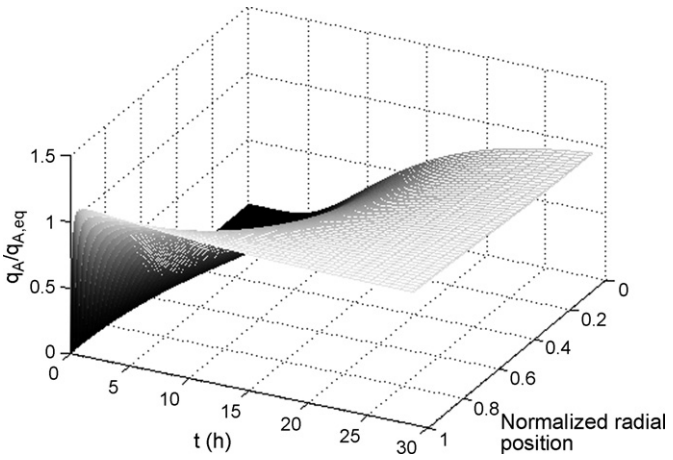

Fig. 6. Simulation results obtained for Exp. 1 (Table 2) graphed as normalized Cd^{2+} concentration inside the particle as function of time and normalized radial position.

to sorbent saturation, which was not observed in this work as Fig. 4 clearly points out.

Fig. 5 provides a comparison between our equilibrium results and others available in the literature for Cd^{2+} removal from aqueous solutions with different materials. For example, Kocaoba et al. [17] compared the performance of Amberlite IR 120 and dolomite at 293 K, El-Kamash et al. [18] studied synthetic zeolite A at 298 K, and Sprynskyy et al. [19] reported data for clinoptilolite at room temperature. The ion-exchange capacity of ETS-4 (this work) is generally larger than that of these materials. Such results emphasise ETS-4 effectiveness to remove Cd^{2+} ions from waste solutions.

With respect to the results obtained with the Nernst–Planck model (lines in Figs. 1 and 2) it may be pointed out the good agreement observed between modelling and measurements, corresponding to AAD = 6.74%. Reliable correlation is accomplished even in the transition from steep descent to the horizontal branch, where kinetic curves are frequently difficult to fit. The intraparticle self-diffusivities and the convective mass transfer coefficient fitted to the experimental data, together with the AADs, are listed in Table 4.

Fig. 6 illustrates the normalized concentration of cadmium(II) in the ETS-4 particles as function of time and radial position, for Exp. 1 of Table 2. Similar behaviour is found for the remaining experiments. This plot confirms expected trends, nonetheless it is interesting to detach the time evolution of normalized concentration at surface, $q_A(t;r=R)/q_{A\infty}$). According to Fig. 6, initial sudden rise of surface concentration is so pronounced that it goes through a maximum and than decreases gradually until equilibrium is reached. Inside particle, far from surface, monotonous behaviour is found instead. With no film resistance, the initial particle concentration at surface would change suddenly from $q_A(t=0^-,r=R)=0$ to $q_A(t=0^+,r=R)=q_A(C_{A0})$, which is the concentration in equilibrium with bulk solution. Then, for $t>0$, $q_A(t,r=R)$ would decrease monotonously until final system equilibration. This figure illustrates such behaviour, but the existence of external diffusion smoothes the ideal trend identified with initial step increase.

Table 4
Calculated results obtained with the Nernst–Planck model: parameters optimized and average absolute deviation

D_A ($m^2\ s^{-1}$)	2.595×10^{-19}
D_B ($m^2\ s^{-1}$)	2.434×10^{-18}
k_f ($m\ s^{-1}$)	1.28×10^{-3}
AAD (%)	6.74

In Fig. 7 the calculated *versus* experimental Cd^{2+} solution concentration are graphed in normalized form. This figure shows the good performance of the proposed NP based model and its superiority over the semiempirical equations also represented, particularly the pseudo first-order one, illustrated by the deviations achieved: $AAD_{NP} = 6.74\%$, $AAD_{1\text{-order}} = 251.7\%$ and $AAD_{2\text{-order}} = 12.11\%$. It should be mentioned that the number of data points is the same for the three models, whereas the number of parameters fitted is different (Nernst–Planck = 3, and pseudo first- and second-order equations is 4).

The diffusion coefficients of Cd^{2+} and Na^+ are 2.595×10^{-19} and $2.434 \times 10^{-18}\ m^2\ s^{-1}$, respectively. The orders of magnitude of our values are consistent with the small pore diameters of ETS-4 (0.3–0.4 nm) and in line with other data found in the literature for microporous exchangers. For instance, apparent diffusion coefficients of 1.8×10^{-17} and $8.0 \times 10^{-18}\ m^2\ s^{-1}$ were obtained by Coker and Rees [27] for Ca^{2+} and Mg^{2+}, respectively, in semi-crystalline zeolite Na-A; Brooke and Rees [28] reported interdiffusion diffusivities in the range of 10^{-18} to $10^{-19}\ m^2\ s^{-1}$ for the system Na^+/K^+ in shabazite; and Coker and Rees [29] reported interdiffusion coefficients of 2.00×10^{-18} and $6.53 \times 10^{-18}\ m^2\ s^{-1}$ for Na^+/Ca^{2+} and Na^+/Mg^{2+} in beryllophosphate. Ahmed et al. [5] published an esti-

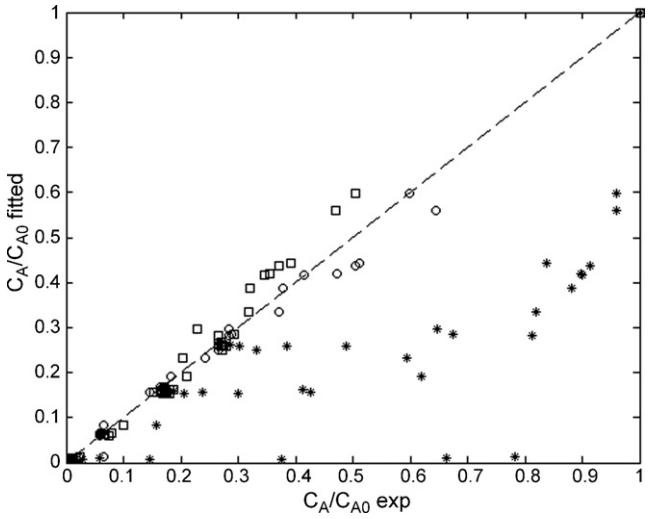

Fig. 7. Plot of the calculated *versus* experimental normalized Cd^{2+} concentrations in bulk solution: Symbols: (○) Nernst–Planck based model of this work; (*) pseudo first-order model; (□) pseudo second-order model.

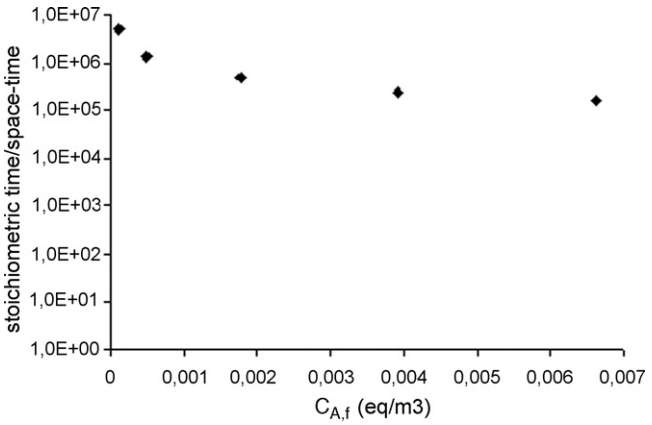

Fig. 8. Ratio between stoichiometric time and space-time plotted for each concentration of the isotherm measured in this work (Fig. 4).

mated Cd^{2+} apparent diffusion coefficient of 2.84×10^{-23} m^2 s^{-1} in CaX zeolite, based on an intraparticle diffusion model neglecting external diffusion resistances. However, the simulation achieved with such coefficient was comparatively poor relatively to that obtained by simply fitting a first-order kinetic model to the experimental data.

Concerning the convective mass transfer coefficient, we obtained $k_f = 1.28 \times 10^{-3}$ m s^{-1}. It is interesting to verify that the correlation of Armenante and Kirwan (Eq. (17)) predicts $k_f = 2.20 \times 10^{-3}$ m s^{-1}. It is a reliable result if one attends to the fact that power is approximately calculated for our experimental set-up, and the size of our ETS-4 particles ($d_p = 0.7 \times 10^{-6}$ m) is one order of magnitude lower than the inferior limit studied by Armenante and Kirwan (range of $d_p = (6–420) \times 10^{-6}$ m).

In practice, separations accomplished with solid agents are often conducted in percolation columns (i.e. fixed-bed), because a nearly solute-free effluent may be obtained until the solid agent in the bed approaches saturation. The large sorption capacity of ETS-4 leads us to estimate the ratio between stoichiometric time (t_{st}) and space-time (τ) of a percolation column, which is an essential parameter for equipment design [30]:

$$t_{st} = \tau \left(1 + \frac{1-\varepsilon}{\varepsilon} \frac{q_{A,f}}{C_{A,f}}\right) \quad (19)$$

Here, $q_{A,f}$ is the solid concentration in equilibrium with the feed concentration $C_{A,f}$, and ε is the bed porosity. In Fig. 8 the ratio t_{st}/τ for each point of our isotherm (Fig. 4) is represented, assuming $\varepsilon \approx 0.5$. As expected, extremely high values (in the range of 10^5 to 10^6) are obtained, which means that the concentration wave front moves through the bed at a velocity that is much lower than the interstitial fluid velocity. Furthermore, since the Freundlich isotherm is of the favourable type, a self-sharpening wavefront arises, hence desirable constant pattern flow develops along bed during loading step. We are presently formulating supported pellets of ETS-4 to study the dynamics of a percolation column to clean cadmium aqueous solutions.

5. Conclusions

The ETS-4 ability to uptake Cd^{2+} ions from aqueous solution has been investigated in batch experiments. This material exhibits a large ion-exchange capacity, and 2 h are sufficient to remove 94% of Cd^{2+} from a solution with initial concentration 0.62×10^{-3} kg/m^3, when 50 g of ETS-4 is used per m^3 of solution.

Freundlich isotherm fitted the equilibrium data accurately. The solid loadings measured in this essay surmount significantly the values reported in the literature for the same set of temperatures (293–298 K), for ion exchangers such as Amberlite IR 120, dolomite, synthetic zeolite A, and clinoptilolite, showing that ETS-4 has considerable potential as a decontaminating agent for waters.

A Nernst–Planck based model combining film and intraparticle diffusion control has been successfully applied to describe the experimental data, where the convective mass transfer coefficient and the self-diffusivities of Cd^{2+} and counter ion Na^+ are the unique parameters. Good representations are accomplished (AAD = 6.74%) even in the transition from the steep descent to the horizontal branch of the C_A/C_{A0} *versus* time curve. The diffusion coefficients of Cd^{2+} and Na^+ are 2.595×10^{-19} and 2.434×10^{-18} m^2 s^{-1}, respectively, consistent with the small-pore size of ETS-4 and agree with the values previously reported for other microporous materials.

Results obtained with NP based model are clearly superior to those of the pseudo first- and second-order models, as evidenced by the deviations found: $AAD_{1\text{-order}} = 251.7\%$ and $AAD_{2\text{-order}} = 12.11\%$).

Acknowledgments

Patrícia F. Lito and Cláudia B. Lopes express their gratitude to Fundação para a Ciência e Tecnologia (Portugal) for the PhD grants provided (SFRH/BD/25580/2005 and SFRH/BD/19098/2004) and FEDER for financial support. We thank Dra. Teresa Caldeira for all support in the analytical part.

References

[1] V.J. Inglezakis, M.D. Loizidou, H.P. Grigoropoulou, Equilibrium and kinetic ion exchange studies of Pb^{2+}, Cr^{3+}, Fe^{3+} and Cu^{2+} on natural clinoptilolite, Water Res. 36 (2002) 2784–2792.
[2] R. Petrus, J. Warchol, Ion exchange equilibria between clinoptilolite and aqueous solutions of Na^+/Cu^{2+}, Na^+/Cd^{2+} and Na^+/Pb^{2+}, Micropor. Mesopor. Mater. 61 (2003) 137–146.
[3] M. Trgo, J. Peric, N.V. Medvidovic, A comparative study of ion exchange kinetics in zinc/lead-modified zeolite–clinoptilolite systems, J. Hazard. Mater. B 136 (2006) 938–945.
[4] B. Biskup, B. Subotic, Kinetic analysis of the exchange processes between sodium ions from zeolite A and cadmium, copper and nickel ions from solutions, Sep. Purif. Technol. 37 (2004) 17–31.
[5] I.A.M. Ahmed, S.D. Yong, N.M.J. Crout, Time-dependent sorption of Cd^{2+} on a CaX zeolite: experimental observations and model predictions, Geochim. Cosmochim. Acta 70 (2006) 4850–4861.
[6] C.B. Lopes, M. Otero, J. Coimbra, E. Pereira, J. Rocha, Z. Lin, A. Duarte, Removal of low concentration Hg^{2+} from natutal waters by microporous and layered titanosilicates, Micropor. Mesopor. Mater. 193 (2007) 325–332.
[7] C.B. Lopes, P.F. Lito, M. Otero, Z. Lin, J. Rocha, C.M. Silva, E. Pereira, A. Duarte, Mercury removal with titanosilicate ETS-4: batch experiments and modelling, Micropor. Mesopor. Mater. 115 (2008) 98–105.
[8] J. Rocha, M.W. Anderson, Microporous titanosilicates and other novel mixed octahedral–tetrahedral framework oxides, Eur. J. Inorg. Chem. (2000) 801–818.
[9] S. Lagergren, About the theory of so-called adsorption of soluble substances, Kungliga Svenska Vetenskapsakademiens. Handlingar 24 (1989) 1–39.
[10] C. Namasivayam, S. Senthilkumar, Removal of arsenic(V) from aqueous solution using industrial solid waste: adsorption rates and equilibrium studies, Ind. Eng. Chem. Res. 37 (1998) 4816–4822.
[11] Y.S. Ho, G. McKay, The sorption of lead(II) ions on peat, Water Res. 33 (1999) 578–584.
[12] F. Helfferich, Ion Exchange, Dover, NY, 1995.
[13] J.F. Rodrígez, J.L. Valverde, A.E. Rodrigues, Measurement of effective self-diffusion coefficients in a gel-type cation exchanger by the zero-length-column method, Ind. Eng. Chem. Res. 37 (1998) 2020–2028.
[14] C.B. Lopes, M. Otero, Z. Lin, C.M. Silva, E. Pereira, J. Rocha, A. Duarte, Removal of mercury from aqueous solutions by ETS-4 microporous titanosilicate: effect of contact time, titanosilicate mass and initial metal concentration, in: Proceedings of the 11th International Conference on Environmental Remediation and Radioactive Waste Management (ICEMM2007), Bruges, Belgium, 2007.
[15] C.B. Lopes, M. Otero, Z. Lin, C.M. Silva, E. Pereira, J. Rocha, A. Duarte, Mercury removal from aqueous solution using ETS-4—kinetic and equilibrium study, submitted for publication.
[16] S.M. Kuznicki, Preparation of small-pored crystalline titanium molecular sieve zeolite, US Patent 4,938,939 (1990). Assigned to Engelhard Corporation.
[17] S. Kocaoba, Comparison of Amberlite IR 120 and dolomite's performances for removal of heavy metals, J. Hazard. Mater. 147 (2007) 488–496.

[18] A.M. El-Kamash, A.A. Zaki, M.A. El Geleel, Modeling batch kintetics and thermodynamics of zinc and cadmium ions removal from waste solutions using synthetic zeolite A, J. Hazard. Mater. B 127 (2005) 211–220.
[19] M. Sprynskyy, B. Buszewski, A.P. Terzyk, J. Namiesnik, Study of the selection mechanism of heavy metal (Pb^{2+}, Cu^{2+}, Ni^{2+}, and Cd^{2+}) adsorption on clinoptilolite, Colloid Interf. Sci. 304 (2006) 21–28.
[20] G.X.S. Zhao, J.L. Lee, P.A. Chia, Unusual adsorption properties of microporous titanosilicate ETS-10 toward heavy metal lead, Langmuir 19 (2003) 1977–1979.
[21] W.E. Schiesser, The Numerical Method of Lines, Academic Press, USA, 1991.
[22] W.H. Lawton, E.A. Sylvestre, Elimination of linear parameters in nonlinear regression, Technometrics 13 (1971) 461–467.
[23] H. Liu, C.M. Silva, E.A. Macedo, Unified approach to the self-diffusion coefficients of dense fluids over wide ranges of temperature and pressure-hard-sphere, square-well, Lennard-Jones and real substances, Chem. Eng. Sci. 53 (1998) 2403–2422.
[24] P.M. Armenante, D.J. Kirwan, Mass transfer to microparticles in agitated systems, Chem. Eng. Sci. 44 (1989) 2781–2796.
[25] M.A. Fernandez, G. Carta, Characterization of protein adsorption by composite silica-polyacrylamide gel anion exchangers. I. Equilibrium and mass transfer in agitated contactors, J. Chromatogr. A 746 (1996) 169–183.
[26] A. Bhattacharya, Predicting rates of dissolution of polydisperse solids in reactive media, Chem. Eng. Process. 46 (2007) 573–583.
[27] E.N. Coker, L.V.C. Rees, Kinetics of ion-exchange in quasi-crystalline aluminosilicate zeolite precursors, Micropor. Mesopor. Mater. 84 (2005) 171–178.
[28] N.M. Brooke, L.V.C. Rees, Kinetics of ion-exchange. Part II. Trans, Trans. Faraday Soc. 65 (1969) 2728–2739.
[29] E.N. Coker, L.V.C. Rees, Ion exchange in beryllophosphate-G, J. Chem. Soc., Faraday Trans. 88 (1992) 273–276.
[30] D.M. Ruthven, Principles of Adsorption and Adsorption Processes, John Wiley & Sons, USA, 1984.